ORIGINAL ARTICLE

Alon Meir · Annette C. Dolphin

Kinetics and Gβγ modulation of Ca$_v$2.2 channels with different auxiliary β subunits

Abstract Modulation of calcium channels by both auxiliary subunits and G proteins was studied in cell-attached patches from COS-7 cells transfected with Ca$_v$2.2 channel subunits (N-type, α_1B and either β_{1b} or β_{2a}). These were co-expressed with either G$\beta_1\gamma_2$ or the Gβγ-binding domain of β-adrenergic-receptor kinase-1 to sequester endogenous Gβγ. Since G protein modulation of Ca$_v$ channels may affect both inactivation and activation, we examined Gβγ modulation of Ca$_v$2.2 channels in the presence of two different β-subunits that affect inactivation differently and compared in detail the single-channel characteristics of N-type channels expressed with either of these β-subunit isoforms. The single-channel mean amplitude and mean open time were not influenced by the transfection combination. However, the mean closed time at +40 mV was increased for both β_{1b} and β_{2a}-subunits by co-transfection with G$\beta_1\gamma_2$. This effect was absent at lower voltages as examined for channels with the β_{1b}-subunit. The distribution of latency-to-first-opening of Ca$_v$2.2 channels was similar for both β-subunit isoforms. However, the inclusion of the β_{2a} subunit resulted in channels with an additional, prominent, slow activation phase. Co-transfection of G$\beta_1\gamma_2$ with Ca$_v$2.2 channels markedly reduced the ensemble current amplitude and slowed the first latency. The inhibition imposed by G$\beta_1\gamma_2$ was largely independent of the β-subunit species. Facilitation of Gβγ-modulated currents (the channel response following a large and brief depolarising prepulse) was observed for channels with both β-subunits and involved mainly enhancement of the activation, as assessed by the faster first latency. The inactivation process was strongly dependent on the β-subunit species, with β_{1b} supporting inactivation and β_{2a} reducing this process. This difference was assessed by estimation of both steady-state inactivation (prepulse influence on test pulse responses) and the inactivation time course during depolarisation. At +40 mV, channels with the β_{1b}-subunit had a fast component of inactivation (time constant ~180 ms, 50%) and a slow phase with time constant of ~1 s, while the β_{2a}-subunit supported only a very slow inactivation process with time constant of ~5 s. Co-transfection of G$\beta_1\gamma_2$ with the Ca$_v$2.2 channel had no effect on the inactivation properties with either β-subunit. In summary, we show that the inactivation properties of expressed Ca$_v$2.2 channels depend largely on the β-subunit species and to a minor extent only on the presence or absence of the Gβγ modulator. Furthermore, the activation, amplitude, mean open and closed times and G protein modulation of N-type channels were similar for both β_{1b}- and β_{2a}-subunits.

Keywords Ca$_v$2.2 · β-Subunit · Gβγ · Activation · Inactivation

A. Meir (✉) · A.C. Dolphin
Department of Pharmacology, University College London,
London WC1E 6BT, UK
e-mail: a.dolphin@ucl.ac.uk
Fax: +44-20-78132808

Present address:
A. Meir, Alomone Labs Ltd., Har-Hotzvim Hi-Tech Park,
P.O. Box 4287, Jerusalem 91042, Israel
e-mail: alon@alomone.com
Tel.: +972-2-5871102, Fax: +972-2-5867675

Introduction

Voltage-dependent calcium (Ca$_v$) channels play an essential role in the control of many cellular processes, including synaptic transmission, by transducing a voltage signal into elevation of intracellular Ca^{2+} [21, 50]. Although capable of generating functional Ca$_v$ channels when expressed alone [27], the pore-forming α_1-subunits interact with auxiliary subunit proteins [53] and form further complexes with other neighbouring proteins.

Four isoforms of the Ca$_v$ channel auxiliary β-subunits have been cloned and shown to be involved in membrane targeting of the putative pore-forming α_1-subunits [5, 6, 16]. In addition, β-subunits modulate the biophysical properties of the Ca$_v$1 [19] and Ca$_v$2 [46, 52] channel families. A common effect of the different β-subunits is to enhance the coupling between depolarisation and acti-

vation and to increase the channel open probability [53]. Finally, the β-subunit plays an important role in shaping the inactivation properties of the channel [45].

Inactivation properties also depend on the expressed Ca_v α_1-isoforms [14, 56] and also on $\alpha_2\delta$-[42] and γ-subunits [7, 29] (for review see [47]). The inactivation process contributes to the duration and magnitude of the calcium signal, so that alterations in inactivation may influence signalling.

In presynaptic nerve terminals, the Ca_v channels most involved in release are members of the Ca_v2 family (also known as α_1A, B and E, for review see [32]). In addition to their interaction with auxiliary subunits, functional and binding assays have shown these channels to interact with syntaxin [2], calmodulin [37] and the guanine nucleotide-binding protein (G protein) βγ-subunit (Gβγ) [23].

The interaction of Ca_v channels with Gβγ forms the basis of G protein-mediated inhibition of transmitter release. This widespread form of inhibitory synaptic modulation involves neurotransmitters such as dopamine, GABA and opiates binding to presynaptic G protein-coupled receptors, liberating activated Gβγ dimers [25] and inhibiting calcium currents [3, 20, 40]. We have shown recently that voltage-dependent inhibition induced by $G\beta_1\gamma_2$ and the associated prepulse facilitation of $Ca_v2.2$ channels requires the presence of a β-subunit [30] and also that the off-rate of Gβγ is enhanced by β-subunits [10, 11].

Interactions between G protein modulation and inactivation have been suggested on the basis of increased apparent inactivation of facilitated currents (see for example [35, 49]). In addition, site-directed mutations in a Gβγ-binding motif on the intracellular loop connecting domains I and II causes changes in the inactivation properties [24]. Nevertheless, it is possible that the alteration in inactivation of mutated α_1 constructs that have modified G protein modulation, is a result of alterations in the influence of the β-subunit. For example, deletions and mutations in the N-terminus of the $Ca_v2.2$ channels have shown that this region contains determinants for G protein modulation [12, 34] and also for β-subunit-dependent inactivation properties [45].

Since the auxiliary β-subunit is involved in both shaping the inactivation and in Gβγ modulation, we examined properties of N-type channels constructed with two different β-subunit isoforms. Whereas the inactivation behaviour of the channel was affected differently by the two β-subunits, other kinetic parameters and modulation by G proteins, which are both dependent on the presence of the auxiliary β-subunit, were affected similarly by the two β-subunits.

Materials and methods

Materials

The following cDNAs were used: rabbit α_{1B} (GenBank accession number D14157), rat β_{1b} (X11394), rat β_{2a} (M80545), bovine $G\beta_1$ (M13236), bovine $G\gamma_2$ (M37183), β-adrenergic-receptor-kinase$_1$ Gβγ-binding domain minigene (called here βARK_1, M34019) and mut3 green fluorescent protein (GFP, [18]). Transfections also included rat $(\alpha_2$-$\delta)_1$ cDNA (M86621 from Dr. H. Chin). All cDNAs were used in the pMT2 vector [48].

Transfection of COS-7 cells

COS-7 cells were cultured and transfected using the electroporation technique. GFP was used as a reporter for successful transfection, essentially as described previously [9, 44].

Single-channel recording

All recordings were performed on GFP-positive cells at room temperature (20–22 °C). Recording pipettes were pulled from borosilicate tubing (WPI, Sarasota, Fla., USA), coated with Sylgard (Sylgard 184, Dow Corning, Wiesbaden, Germany) and fire polished to form high-resistance pipettes (~10 MΩ with 100 mM $BaCl_2$). The bath solution, designed to clamp the resting membrane potential at zero [31], comprised (in mM): 135 K-aspartate, 1 $MgCl_2$, 5 EGTA and 10 HEPES (titrated with KOH, pH: 7.3). Patch pipettes were filled with a solution of the following composition (in mM): 100 $BaCl_2$, 10 tetraethylammonium (TEA)-Cl, 10 HEPES, 0.0002 tetrodotoxin (TTX), titrated with TEA-OH to pH: 7.4. Both solutions were adjusted to 320 mOsmol with sucrose. Data were sampled (Axopatch 200B and Digidata 1200 interface, Axon Instruments, Union City, Calif., USA) at 5–10 kHz and filtered on-line at 1 kHz. Voltages were not corrected for the liquid junction potential [33], measured to be –15 mV in these solutions, to allow comparison of the results with other published data.

Single-channel analysis

Leak subtraction was performed by averaging segments of traces with no activity from the same voltage protocol in the same experiment, and subtracting this average from each episode using pClamp (v. 6, Axon Instruments). Events were detected using the half-amplitude threshold method. Single-channel amplitude was determined by a Gaussian fit to the binned amplitude distributions. Open (t_{open}) and closed (t_{closed}) times were measured either in single-channel patches or in stretches of activity between the two last inactivation events, in which only a single channel was active (see below and Fig. 6a). The distributions of t_{open} and t_{closed} were fitted with double exponential functions and the mean calculated by summing the weighted short and long time constants (Fig. 2b). To establish whether this way of calculating the mean t_{closed} was accurate, we compared the closed-time analysis for one, two and three channels in the patch and found the mean values to be very similar (Fig. 2d).

Data are expressed as mean±SEM. The significance of differences between means was established using Student's t-test for paired or unpaired samples as appropriate.

The ensemble current recorded from a membrane patch (I) was considered to be a function of the number of channels in the patch (N), the single-channel current (i) and the single channel open probability (P_{open}) according to:

$$I = NiP_{open} \tag{1}$$

N was estimated as described below. The single-channel current i is a function of the single-channel conductance γ and the electrochemical driving force for the permeating ions, which is the difference between the membrane voltage (V) and the channel reversal potential ($V_{reversal}$). Both γ and $V_{reversal}$ are dependent on the $[Ba^{2+}]$, which was constant in these experiments. In addition, γ depends on an intrinsic divalent ion binding ability of the channel. P_{open} depends on the probability of activation, the probability of inactivation and on the mean t_{open} and t_{closed}. We assumed that t_{open} and t_{closed} were constant for the duration of a given voltage pulse.

Patches with run-down were not included, since the estimated number of channels in a patch is an influential parameter in this analysis. Run-down was examined by comparing ensemble currents taken at different time points during an experiment.

Estimation of the number of channels in the patch

The maximal detected number of superimposed openings may represent the number of channels in the patch (see [30]). The accuracy of such estimation increases with increasing channel P_{open} and decreasing N. To be able to use such an estimation in our analysis we took the following measures: we examined the presence of overlapping openings at +40 mV, which is near the peak of the I/V relationship. In addition we used very long pulses (2 s), both to extend the maximal P_{open} window and for measuring t_{closed} (see above). Moreover, we restricted all the single-channel analysis to patches with no more than three overlapping openings.

Latency analysis

Latency-to-first-opening (FL) was measured in 2-ms bins and the numbers of latency events (as measured in at least 20 consecutive episodes) were plotted as a function of the latency. If necessary, their distribution was corrected for N (see below). FL histograms were normalized and accumulated according to:

$$P_{FL}=\sum_0^t \frac{N_{FL}}{n_T} \qquad (2)$$

where N_{FL} is the number of first-latency events and P_{FL} the normalised-cumulative first latency distribution (N and P stand here for the number of events and the probability, respectively, see below). The N_{FL} distribution was divided by the total number of episodes collected (n_T) to give the probability that the latency equals t ms. The distributions were then accumulated to express the probability that the latency is equal to or less than t ms [26].

Correction for the number of channels was performed as described in [30, 36] according to:

$$P_{FL,1}=1-(1-P_{FL,N})^{\frac{1}{N}} \qquad (3)$$

where $P_{FL,N}$ and $P_{FL,1}$ represent the original (multi-channel) and corrected (single-channel) latency distributions respectively. At all voltages we measured P_{FL} at $t=20$ ms (the mean of the ten points between 10 and 30 ms) and at +40 mV we also fitted P_{FL} distributions with either a single or a double exponential function to allow estimation and comparison of the activation kinetics:

$$P_{FL}=Y_0+Ae^{-\frac{t}{\tau}} \qquad (4)$$

or

$$P_{FL}=Y_0+A_{fast}e^{-\frac{t}{\tau_f}}+A_{slow}e^{-\frac{t}{\tau_s}} \qquad (5)$$

where Y_0 is the fraction of channels activating, A the relative weight, t and τ the time and the time constant respectively and the subscripts fast (f) and slow (s), indicate the fast and the slow time courses respectively.

Inactivation measurements

Prepulse inactivation

We examined the effect of a 2-s prepulse and measured both the ensemble current amplitude and the latency-to-first-opening, in the test pulse.

Inactivation during 2-s pulse to +40 mV

This analysis is based on measuring the time at which the last closure (LC) in a 2-s episode occurs (in 50-ms bins). Since the LC in the 2-s episode was always registered, we also included all the episodes in which inactivation was not detected (with LC value of 2000 ms). This analysis includes the assumption that every final transition to a lower level (in multi-channel patches) is an inactivation event. Therefore, events were gathered from the termination times of dwelling at each level. This assumption was tested by calculating the probability of two channels being active simultaneously, without detecting simultaneous, overlapping openings, in all the stretches of activity between the transition from level 2 to 1 and from level 1 to baseline according to:

$$n_2=n_T \frac{t_{open}}{2\,t_{closed}} \qquad (6)$$

where n_2 is the expected number of double openings and n_T the total number of events. In all the stretches of activity tested, the observed n_2 was 0. Since the combination of high P_{open} and lack of double openings in these stretches suggests strongly that only one channel is active (see for example [17]), we conclude that the last closure leading to this stretch was also an inactivation event. All the detected inactivation events were summed, divided by the number of detected events (n_i) and accumulated to express the time course of inactivation, given that the channel has opened:

$$P_{LC}=\sum_0^t \frac{N_{LC}}{n_i} \qquad (7)$$

where N_{LC} and P_{LC} are the last closure and cumulative last closure distributions and n_i is the number of detectable inactivation events. The P_{LC} distribution at +40 mV was fitted with a single (β_{2a}) or double (β_{1b}) exponential in which $Y_0=-1$ and either A or ($A_{fast}+A_{slow}$)=1 (as in Eqs. 4 and 5 respectively). This method introduces an error into the analysis due to the final period after the last registered inactivation event. It may be part of a long closed state that was truncated by the termination of the pulse (introducing a sharp artefactual drop at the end of the pulse, see also Fig. 6a). To avoid errors arising from long closed states at the end of the episode and from the non-inactivating fraction, we chose to fit the range 0–1850 ms (38 out of the 41 points in the range 0–2000 ms) because there were few closures longer than 150 ms (Fig. 2).

Results

Single-channel activity was recorded at several patch potentials, from cells transfected with $Ca_v2.2$ and $\beta_{1b}/\beta ARK_1$, $\beta_{1b}/G\beta_1\gamma_2$, $\beta_{2a}/\beta ARK_1$ and $\beta_{2a}/G\beta_1\gamma_2$ (Fig. 1a–d respectively). The mean ensemble activity in a patch was estimated by averaging leak-subtracted ensemble currents from different patches of the same transfection composition (Fig. 1e). In Fig. 1a–d, examples of four patches with similar estimated number of channels are presented for comparison. Mean I/V relations were then drawn (Fig. 1f). This crude analysis points to several features, including differences in inactivation (see Fig. 1e) that were then studied in detail (see below). At +40 mV, the mean amplitude 20 ms after the onset of the test pulse, in patches from cells co-transfected with βARK_1 was about 2 pA, while in those co-transfected with $G\beta_1\gamma_2$ it was less than 1 pA. The use of long (2-s) pulses in this study (Fig. 2a) enabled accurate measurements of t_{open} and t_{closed} (see Materials and methods and Fig. 2b and c) as well as inducing inactivation that could be examined in detail (see below).
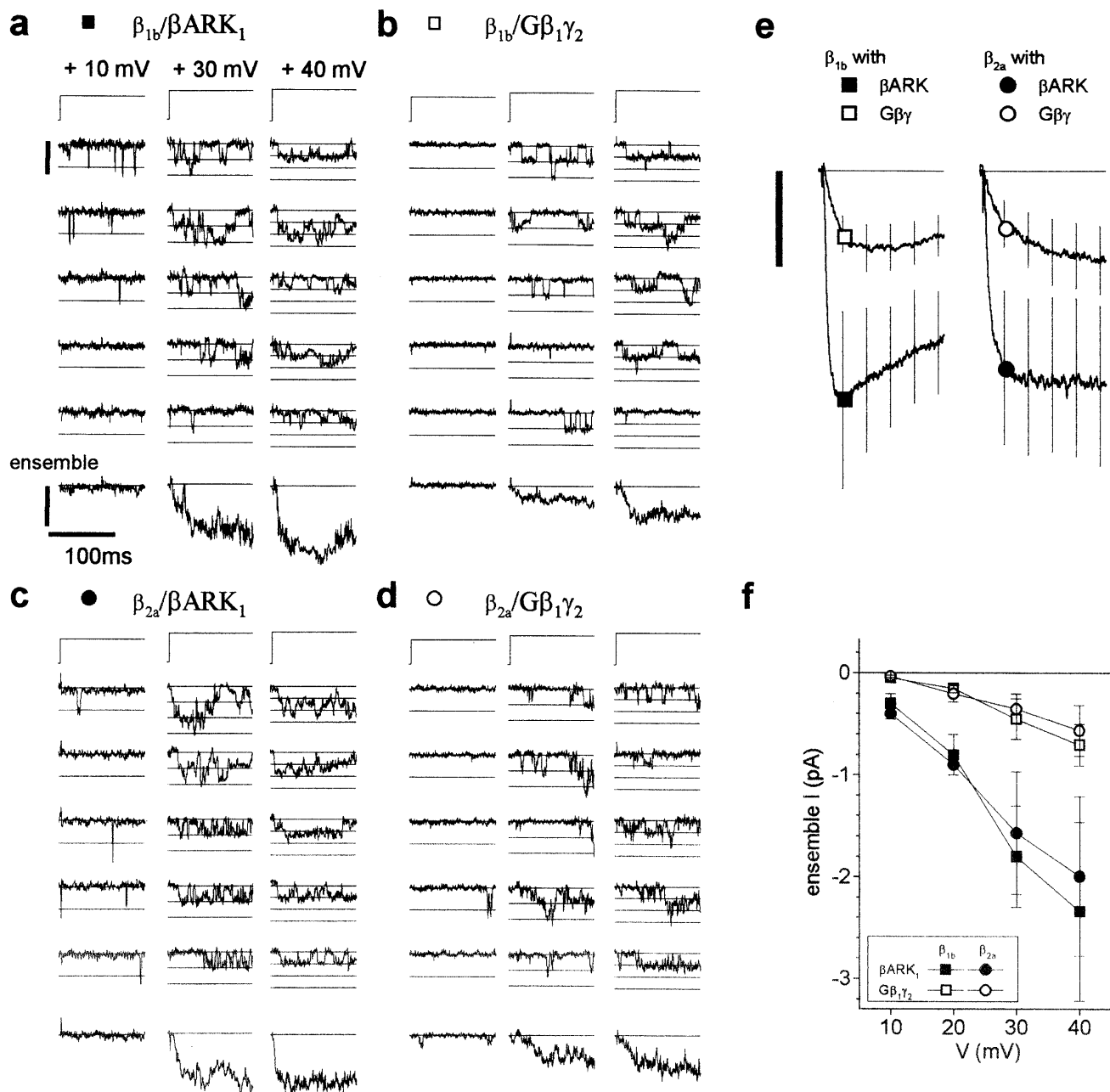
Fig. 1a–f Single-channel and ensemble current for voltage-dependent calcium ($Ca_v2.2$) channels expressed in COS-7 cells with either the β_{1b}- or β_{2a}-subunit and in the presence of the G protein subunit $G\beta_1\gamma_2$ or in the latter's absence [ensured by co-expression of the $G\beta\gamma$-binding domain of β-adrenergic-receptor kinase-1 (βARK_1)]. **a** A representative patch from a cell transfected with $Ca_v2.2/\beta_{1b}$ and βARK_1. The initial 100 ms (in a 2-s test pulse) are shown at three voltages, denoted above each *column* (applies also to **b**, **c** and **d**). *Top*: the voltage protocol, holding potential –100 mV. A 2-s pulse to the indicated voltage is delivered every 10 s. *Middle*: five examples of the response of this patch (openings are *downwards* deflections). *Bottom*: the ensembles of 20 episodes for +10, +30 and +40 mV. The *scale bars* represent 100 ms and 1 pA (to the *left* of the first trace) and 0.5 pA (*bottom*) for the single episodes and ensemble current respectively. The number of open levels that are noted in the *right* column (+40 mV) represents the maximum number of overlapping openings observed in the patch. **b** A representative patch from a cell transfected with $Ca_v2.2/\beta_{1b}/G\beta_1\gamma_2$. Same format as in **a** showing the ensemble of 20, 25 and 20 episodes for +10, +30 and +40 mV respectively. **c** A representative patch from a cell transfected with $Ca_v2.2/\beta_{2a}/\beta ARK_1$. Same format as in **a** showing the ensemble of 18, 11 and 15 episodes for +10, +30 and +40 mV respectively. **d** A representative patch from a cell transfected with $Ca_v2.2/\beta_{2a}/G\beta_1\gamma_2$. Same format as in **a** showing the ensemble of 15, 15 and 20 episodes for +10, +30 and +40 mV respectively. **e** Mean (±SEM, shown every 20 ms for clarity) ensemble currents at +40 mV (100 ms) for β_{1b} (*left*) and β_{2a} (*right*), number of experiments as in **f** (see below). The *vertical bar* represents 1 pA. **f** Mean ensemble current (taken 20 ms after the onset of the voltage pulse) as a function of the voltage step for $Ca_v2.2$ channels co-expressed with $\beta_{1b}/\beta ARK_1$ (■, $n=12$), $\beta_{1b}/G\beta_1\gamma_2$ (□, $n=24$), $\beta_{2a}/\beta ARK_1$ (●, $n=11$) or $\beta_{2a}/G\beta_1\gamma_2$ (○, $n=11$)
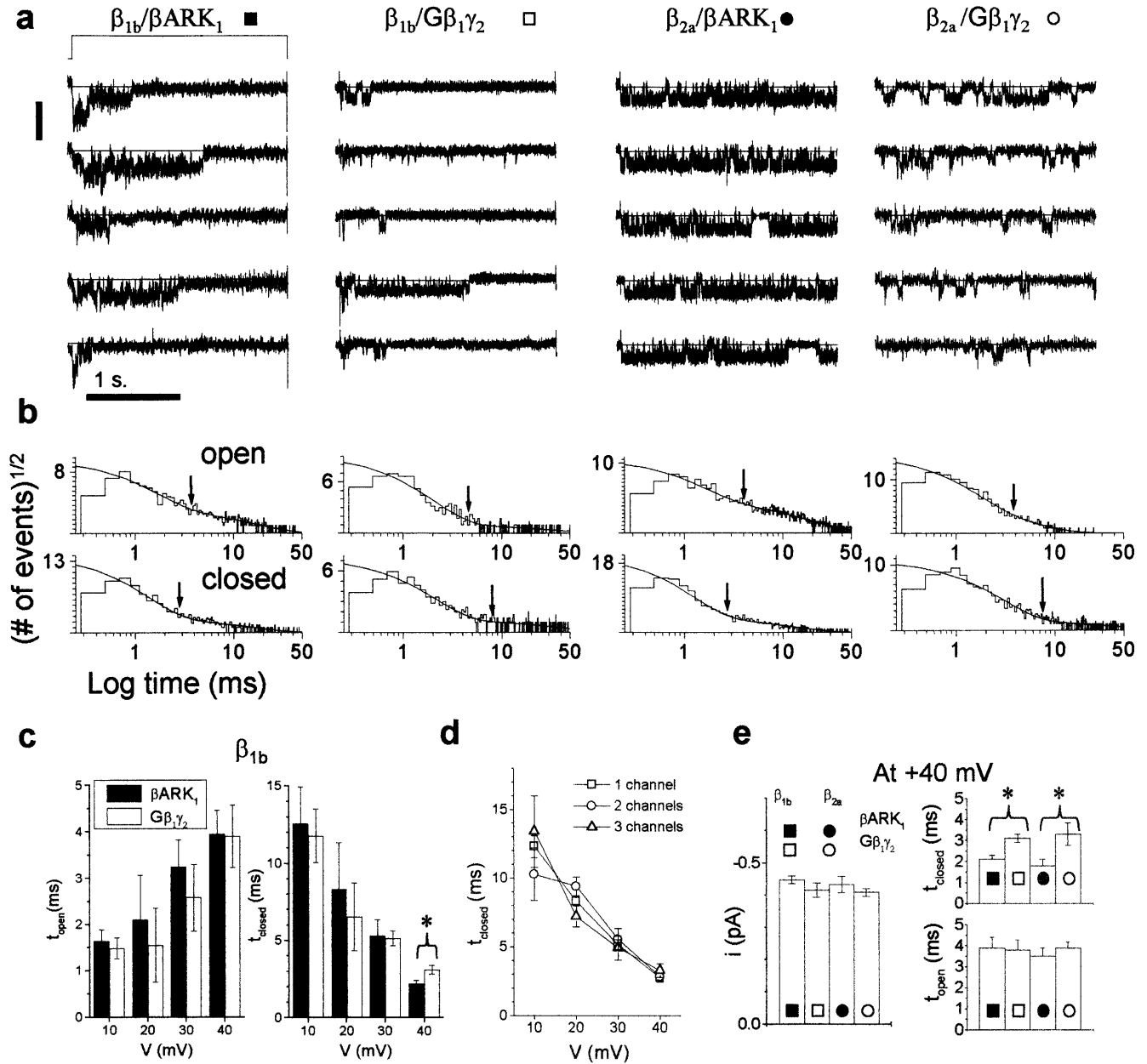
Fig. 2a–e Open and closed times of $Ca_v2.2$ channels with different β-subunits and G proteins. **a** Five examples of 2-s traces to illustrate the detection and analysis of mean closed and open times (see Materials and methods). The extracts of activity that were used in this analysis are either patches with no detectable overlapping openings, or at the end of pulses where only one channel remains active. The subunit composition is denoted on the *top*. The number of overlapping openings in these experiments were (from *left*), three, two, one and two. **b** Open (*top row*) and closed (*bottom row*) time histograms and double exponential fits for each subunit composition from the experiments shown in **a**. *Arrows* mark the calculated mean open and closed times in these experi-ments, closed times were: 2.5, 7.9, 2.6 and 6.9 ms, for $β_{1b}/βARK_1$, $β_{1b}/Gβγ$, $β_{2a}/βARK_1$ and $β_{2a}/Gβγ$, respectively. The mean open time for these compositions was 3.5, 4.2, 3.8 and 3.6 ms respectively. **c** Voltage dependence of mean open (*left*) and closed (*right*) times of the $β_{1b}$-subunit. For $βARK_1$, $n=9$ and for $Gβ_1γ_2$, $n=13$: *$P>0.05$. **d** Examination of mean closed times for patches with one ($n=3$), two ($n=5$) or three ($n=5$) channels, from cells transfec-ted with $Ca_v2.2/β_{1b}/Gβ_1γ_2$. **e** Mean amplitude (*left*) and mean closed (*upper right*) and open (*lower right*) times at +40 mV for both β-subunits (see also Table 1, the numbers of experiments are shown in the table). The data for the $β_{1b}$ subunit at +40 mV from **c** is shown for comparison

Amplitude and steady-state kinetics of $Ca_v2.2$ channels

The single-channel amplitude i at +40 mV was similar for all subunit compositions tested (Table 1, Fig. 2e, left), with a mean value of about 0.4 pA. The ensemble currents, mentioned above, showed a threefold reduction in amplitude in the presence of $Gβ_1γ_2$ (Fig. 1e). The basis for this inhibition may be either a decrease in the number of channels in an average patch or an effect on single-channel properties such as a shorter t_{open}, a

Table 1 Single channel parameters at +40 mV for voltage-dependent calcium (Ca$_v$2.2) channels co-expressed in COS-7 cells with either β$_{1b}$- or β$_{2a}$-subunits, and in the presence of the G protein subunit Gβ$_1$γ$_2$ or in the latter's absence [ensured by co-expression of the Gβγ-binding domain of β-adrenergic-receptor kinase-1 (βARK$_1$)]. (mean I_{patch}, mean ensemble current in a patch, n number of measurements, i single-channel current, t_{open}, t_{closed} channel open and closed times, respectively, τ time constant, act activation, $inact$ inactivation). Means±SEM

Subunits: Ca$_v$2.2 and:	mean I_{patch} (pA)	n	Biophysical properties				Activation					Inactivation				
			i (pA)	t_{open} (ms)	t_{closed} (ms)	n	$\tau_{act-fast}$ (ms)	% fast	$\tau_{act-slow}$ (ms)	% slow	n	$\tau_{inact-fast}$ (ms)	% fast	$\tau_{inact-slow}$ (s)	% slow	n
β$_{1b}$ βARK$_1$	-2.34±0.88	12	-0.45±0.02	3.9±0.5	2.2±0.2[a]	9	12.2±2.1[c]	64±6[e]	171±24	10±4[g]	7	242±57	52±13	0.95±0.2[i]	48±13[k]	7
Gβ$_1$γ$_2$	-0.71±0.20	24	-0.42±0.02	3.9±0.7	3.1±0.3[a]	13	20.0±2.6[c]	50±6[e]	188±62	6±4[h]	10	132±20	50±9	1.04±0.2[i]	50±9[l]	10
β$_{2a}$ βARK$_1$	-2.0±0.78	11	-0.43±0.03	3.5±0.2	2.0±0.2[b]	5	8.3±2.0[d]	61±9[f]	121±14	30±8[g]	6	–	0	4.76±1.2[i]	100[k]	5
Gβ$_1$γ$_2$	-0.56±0.25	11	-0.41±0.01	3.6±0.3	3.3±0.5[b]	5	22.8±5.9[d]	38±7[f]	208±48	32±7[h]	6	–	0	4.83±0.8[i]	100[l]	7

Values assigned the same superscript ([a], [b], [c], etc.), in the same column are significantly different (Student's t-test, $P<0.05$). [a–f]: differences related to Gβγ effects; [g–l]: differences between β$_{1b}$ and β$_{2a}$

longer t_{closed}, slower activation or increased inactivation.

Using only patches that exhibited no more than three overlapping openings at +40 mV, we measured and compared the mean t_{open} and t_{closed} (see Materials and methods). For Ca$_v$2.2 channels with either the β$_{1b}$- or β$_{2a}$-subunit, mean t_{open} was similar, regardless of βARK$_1$ or Gβ$_1$γ$_2$ co-transfection, at all voltages examined (Table 1, Fig. 2c). The t_{open} distributions were fitted with either a double or single exponential (see Fig. 2b and Materials and methods). In all cases mean t_{open} was voltage dependent and in the range of several milliseconds (Fig. 2c and d). The t_{closed} distributions were also fitted with a double exponential (Fig. 2b). Mean t_{closed} showed a steep voltage dependence (Fig. 2c right) and at low voltages was very similar for all the combinations examined. Gβ$_1$γ$_2$ increased mean t_{closed} only at +40 mV (Table 1 and Fig. 2b and e). The possible mechanism for such an influence is discussed below. A long t_{closed} in multi-channel patches may be attributed to gaps between bursts of activity generated by different channels [15]. This analysis confirms a behaviour pattern of the channel in which the channel activates for a single burst and then inactivates. However, we based our analysis on the assumption that in the last stretch of activity, only one channel is active (see Materials and methods) and therefore the differences in mean t_{closed} reflect the effect of Gβ$_1$γ$_2$ and are not an error arising from analysis of multi-channel patches. This was the only difference regarding the steady-state activity of Ca$_v$2.2 channels with Gβγ. Ca$_v$2.2 channels with either β$_{2a}$ or β$_{1b}$ showed very similar properties with respect to the steady-state activity of the channels.

Activation

Ca$_v$2.2 channels activated voltage dependently almost independently of which β-subunit was co-expressed (Figs. 1 and 3). The P_{FL} function (Eq. 2), which describes the time dependence of the FL probability, provides information regarding two processes: the speed of activation and the fraction of channels that do not open (nulls). Figure 3a and b shows P_{FL} distributions and typical traces at different voltages for a single channel from a β$_{2a}$/βARK$_1$ patch (Fig. 3a) and a β$_{2a}$/Gβγ patch (Fig. 3b, maximum three overlapping openings). This procedure was used to estimate the activation for all transfection combinations (Fig. 3c). The voltage dependence of activation at 20 ms was then examined (Fig. 3d). At +40 mV the activation process was characterised further by fitting one or two exponentials to P_{FL} distributions (Fig. 3e). This shows that the activation was compound, comprising mainly a fast process with the β$_{1b}$-subunit and both fast and slow processes with the β$_{2a}$-subunit. Comparison of the responses in Fig. 3 a and b demonstrates the influence of tonic inhibition by Gβ$_1$γ$_2$. The ensemble current was reduced by about 50% (Fig. 1e and f) because of attenuation of the activation.
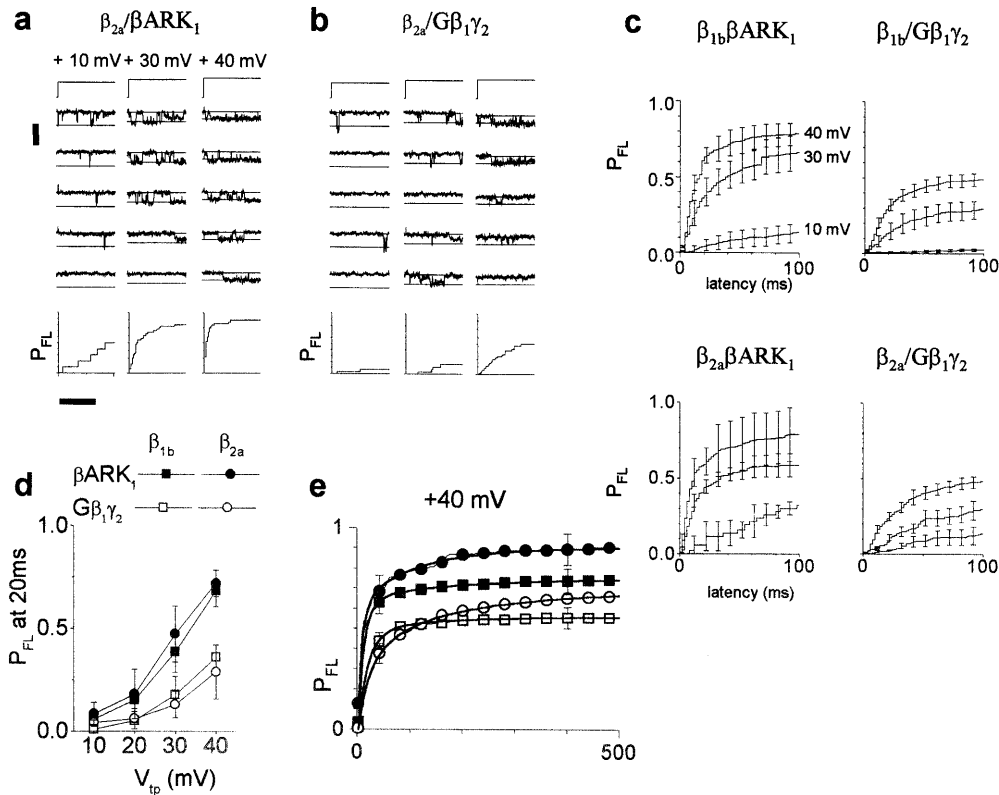
Fig. 3a–e $G\beta_1\gamma_2$ and β-subunit isoforms influence the latency-to-first-opening (*FL*) in $Ca_v2.2$ channels. **a** A representative single-channel patch from a cell transfected with $Ca_v2.2/\beta_{2a}/\beta ARK_1$. The initial 100 ms are shown to demonstrate activation at three voltages (*columns*, applies also to **b**). The voltage protocol is as in Fig. 1. Five examples of the response of this patch and the normalised, cumulative probability function (P_{FL}) collected from 15, 40 and 40 episodes for +10, +30 and +40 mV respectively. The *scale bars* represent 100 ms and 1 pA (to the *left* of the first trace). (**b**) A representative patch from a cell transfected with $Ca_v2.2/\beta_{2a}/G\beta_1\gamma_2$ (maximum of three overlapping openings). Same format as in **a**. At the *bottom*: P_{FL} collected from 15, 15 and 40 episodes for +10, +30 and +40 mV respectively. For this patch with three overlapping openings the distribution of P_{FL} is corrected according to Eq. 3. (**c**) Mean P_{FL} responses (first 100 ms) to voltage pulses to +10, +30 and +40 mV. Means (±SEM marked every 10 ms for clarity). The data was extracted from 9, 11, 6 and 8 experiments for $Ca_v2.2/\beta_{1b}/\beta ARK_1$, $Ca_v2.2/\beta_{1b}/G\beta_1\gamma_2$, $Ca_v2.2/\beta_{2a}/\beta ARK_1$ and $Ca_v2.2/\beta_{2a}/G\beta_1\gamma_2$ respectively. (**d**) Summary of the voltage dependence of the latency-to-first-opening 20 ms after the onset of the pulse for the same compositions. (**e**) The latencies at +40 mV for the compositions shown *above* are superimposed and shown on a 500-ms scale to highlight the long latency component in β_{2a}-containing channels (*n* as in **c**, *symbols* as in **d**). The *bold lines* show the double exponential fits and their values are given in Table 1

Figure 3 summarises the differences in the activation process. During the short period following the onset of the test pulse, the β-subunit species had little influence on activation (Fig. 3c and d). On this time scale, $G\beta_1\gamma_2$ reduced the currents with both β-subunits similarly. However, $Ca_v2.2$ channels with β_{2a} also exhibited a slow activation phase that was absent in β_{1b}-containing channels. The slow activation remained intact during $G\beta_1\gamma_2$ inhibition (Fig. 3e). The P_{FL} functions at +40 mV for

each experiment were fitted with a single or double exponential (Eqs. 4 and 5). Generally, a $\tau_{act\text{-}fast}$ of 8–26 ms, a $\tau_{act\text{-}slow}$ of about 120–210 ms and a null fraction described the activation at +40 mV for all the compositions (Table 1). Significant slowing of $\tau_{act\text{-}fast}$ by $G\beta_1\gamma_2$ was detected with both β-subunits. In addition, the slow component of activation was significantly more pronounced with the β_{2a}-subunit and was not significantly slowed by $G\beta_1\gamma_2$ co-expression (Fig. 3e and Table 1).

Inactivation with different β-subunits

Steady-state inactivation was examined by applying a 2-s prepulse to different potentials and examining the activity in a subsequent 100-ms test pulse to +40 mV (Figs. 4 and 5). Figure 4a and b shows examples of two patches with $Ca_v2.2/\beta_{1b}/G\beta_1\gamma_2$ and $Ca_v2.2/\beta_{2a}/G\beta_1\gamma_2$ respectively. The test pulse was preceded by 2 s at –80 mV (left) or at +40 mV (right). Ensemble currents were generated from experiments of this sort (Fig. 4a and b, last trace and Fig. 4c) and after normalisation, the voltage dependence of the relative inactivation was assessed (Fig. 4d). The β-subunit defined the inactivation properties, but no significant differences in the inactivation process were detected with $G\beta_1\gamma_2$ replacing βARK_1 (Fig. 4d). Measuring FL in the test pulse (Fig. 5) was also used to assess the inactivation due to a long prepulse. With the β_{1b}-subunit, P_{FL} values in the test pulse were reduced following positive prepulse voltages (i.e. V=0 mV) both with βARK_1 and $G\beta_1\gamma_2$ (Fig. 5a). In contrast, with the β_{2a}-subunit, because of the lack of inacti-
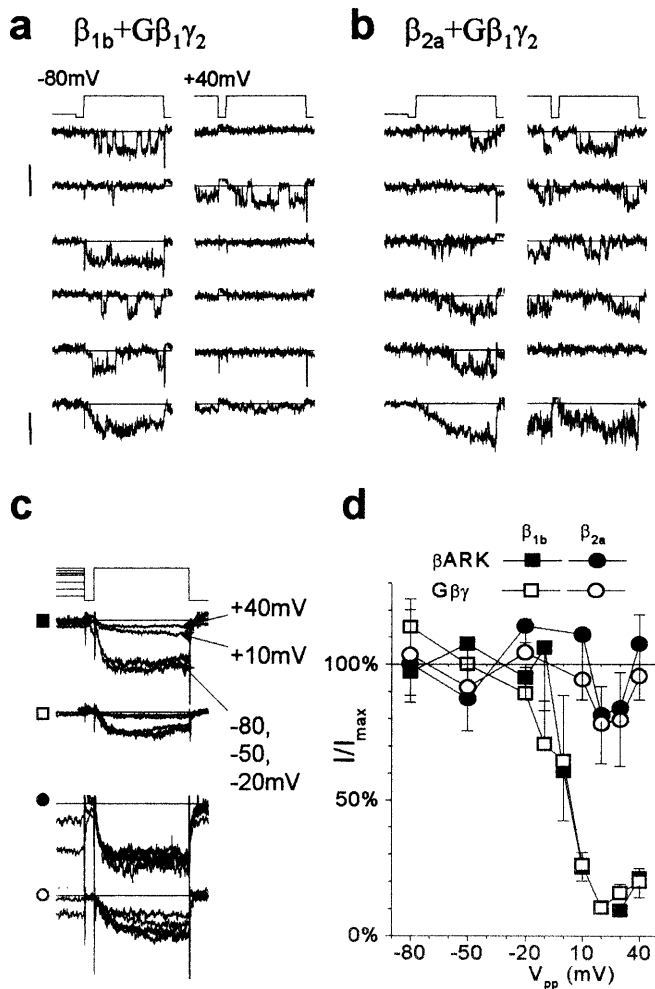
Fig. 4a–d Steady-state inactivation of $Ca_v2.2$ in single- and multi-channel ensemble records. **a** Example traces in response to a 100-ms, +40-mV test pulse preceded by a 2-s prepulse to either –80 mV (*left*) or +40 mV (*right*). The voltage protocol (*top*, holding potential –100 mV) is followed by five consecutive responses recorded from a cell transfected with $Ca_v2.2/\beta_{1b}/G\beta_1\gamma_2$ (with a maximum of three overlapping openings). The *bar* represents 1 pA and applies also to **b**. *Bottom*: an ensemble from the same experiment constructed of 20 episodes at both prepulse potentials. The *bar* represents 0.25 pA and applies to also to **b** and **c**. **b** Example traces recorded from cell transfected with $Ca_v2.2/\beta_{2a}/G\beta_1\gamma_2$ (maximum of three overlapping openings). *Bottom*: an ensemble from the same experiment constructed of 40 and 20 episodes for prepulses to –80 mV and +40 mV respectively. **c** Ensemble average current responses to a test pulse following a 2-s prepulse to –80, –50, –20, +10 and +40 mV (protocol shown on *top*), for the indicated subunit composition (*n* and symbols as in **d**, following). **d** Summary of steady-state inactivation of the ensemble cur-rent level for the four compositions in **c**. All currents were normalised to the mean responses at –80, –50 and –20 mV in each experiment. Combinations: $Ca_v2.2/\beta_{1b}/\beta ARK_1$ (■, *n*=10), $Ca_v2.2/\beta_{1b}/G\beta_1\gamma_2$ (□, *n*=16), $Ca_v2.2/\beta_{2a}/\beta ARK_1$ (●, *n*=8) and $Ca_v2.2/\beta_{2a}/G\beta_1\gamma_2$ (○, *n*=10)

Fig. 5a, b Steady-state inactivation of $Ca_v2.2$ channels in latency records. **a** Reflection of steady-state inactivation in the measurements of latencies, during a test pulse following a 2-s conditioning prepulse of –80 mV or +40 mV (as indicated) for the $Ca_v2.2/\beta_{1b}$ combinations with βARK_1 (*left*, *n*=6) or $G\beta_1\gamma_2$ (*middle*, *n*=10). *Right*: the prepulse voltage (V_{pp}) dependence of P_{FL} 20 ms after the onset of the test pulse. **b** Steady-state inactivation reflected in the measurements of latencies for the $Ca_v2.2/\beta_{2a}$ combinations with βARK_1 (*left*, *n*=8) or $G\beta_1\gamma_2$ (*middle*, *n*=9). Format as in **a**

vation during the conditioning prepulse, the response was fairly constant regardless of the prepulse (Fig. 5b).

Inactivation events can be detected during the 2-s pulses to depolarised potentials (see Methods, Fig. 6a). These events are reflected in the ensemble currents (Fig. 6a, bottom traces and 6b). Summation and normalisation of the inactivation events produced P_{LC} (see Eq. 7), which represents the decay in probability of avoiding inactivation with time. The P_{LC} distributions, measured at +40 mV (see Materials and methods, Fig. 6c), were fitted with one exponential for β_{2a}-containing channels and with a double exponential for β_{1b}-containing channels (Table 1). $Ca_v2.2/\beta_{2a}$ channels inactivated with an estimated $\tau_{inact-slow}$ of 5 s, while $Ca_v2.2/\beta_{1b}$ channels inactivated much faster (Fig. 6b and c). Inactivation of $Ca_v2.2/\beta_{1b}$ channels could be best described by two equally weighted time constants: a $\tau_{inact-fast}$ of 100–200 ms and a $\tau_{inact-slow}$ of about 1 s. $G\beta_1\gamma_2$ had no significant effect on the time course of inactivation in these two conditions (Table 1 and Fig. 6).

Short prepulse facilitation

Voltage-dependent facilitation of $G\beta_1\gamma_2$-modulated channels is dependent on the presence of an auxiliary β-sub-
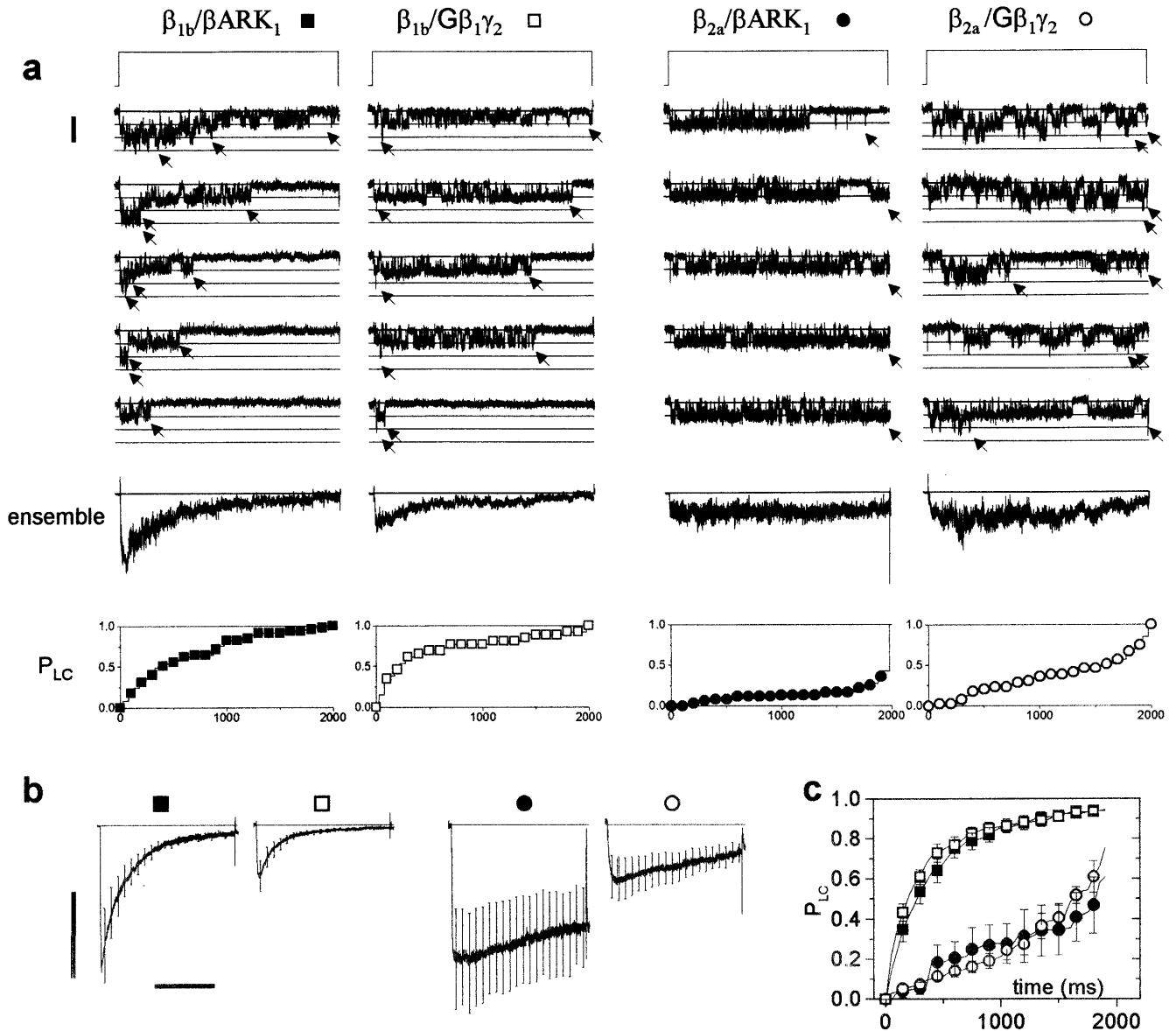
Fig. 6a–c Inactivation of $Ca_v2.2$ channels during 2-s depolarisation to +40 mV. **a** Examples of activity over 2 s at +40 mV for $Ca_v2.2/\beta_{1b}/\beta ARK_1$ (■, maximum of three overlapping openings), $Ca_v2.2/\beta_{1b}/G\beta_1\gamma_2$ (□, maximum of three overlapping openings), $Ca_v2.2/\beta_{2a}/\beta ARK_1$ (●, single channel patch) and $Ca_v2.2/\beta_{2a}/G\beta_1\gamma_2$ (○, maximum of three overlapping openings). Each *column* shows the voltage protocol at the *top* followed by five responses and the ensemble of 20 responses (as in Fig. 2). At the *bottom* the cumulative probability function for the last closure (P_{LC}) is plotted for the same experiment (see Materials and methods). *Diagonal arrows* mark the last closures. The *scale bar* represents 1 pA. **b** Mean single-channel ensemble currents for (from *left* to *right*), $Ca_v2.2/\beta_{1b}/\beta ARK_1$ (*n*=10), $Ca_v2.2/\beta_{1b}/G\beta_1\gamma_2$ (*n*=16), $Ca_v2.2/\beta_{2a}/\beta ARK_1$ (*n*=8) and $Ca_v2.2/\beta_{2a}/G\beta_1\gamma_2$ (*n*=10). The *bars* represent 0.1 pA and 1 s. **c** Mean normalised inactivation during a 2-s prepulse (P_{LC}, see Materials and methods) for $Ca_v2.2/\beta_{1b}/\beta ARK_1$ (■, *n*=7), $Ca_v2.2/\beta_{1b}/G\beta_1\gamma_2$ (□, *n*=10), $Ca_v2.2/\beta_{2a}/\beta ARK_1$ (●, *n*=5) and $Ca_v2.2/\beta_{2a}/G\beta_1\gamma_2$ (○, *n*=8), see Table 1 for fit values

unit [30, 39]. In the present study this was examined by applying a large prepulse (+120 mV for 40 ms) before testing the response of the channels at different voltages (Fig. 7). For both $Ca_v2.2/\beta_{1b}$ (Fig. 7a) and $Ca_v2.2/\beta_{2a}$ (Fig. 7b), at +30 mV, activation was estimated by fitting a double exponential ($\tau_{act-fast}$ and $\tau_{act-slow}$) to the latency plots with and without a prepulse (Fig. 7d). With both β-subunits, $\tau_{act-fast}$ was significantly reduced when preceded by a prepulse. $\tau_{act-fast}$ for β_{1b} and β_{2a} was reduced from 23.9±3.5 and 25.5±2.0 to 12.6±2.0 and 13.3± 2.0 ms respectively. In contrast, $\tau_{act-slow}$, t_{open} and t_{closed} were hardly influenced by the prepulse (Fig. 7c).

Discussion

We employed an approach that facilitated the detailed examination of, and comparison between, calcium channel currents recorded from cell-attached patches of trans-
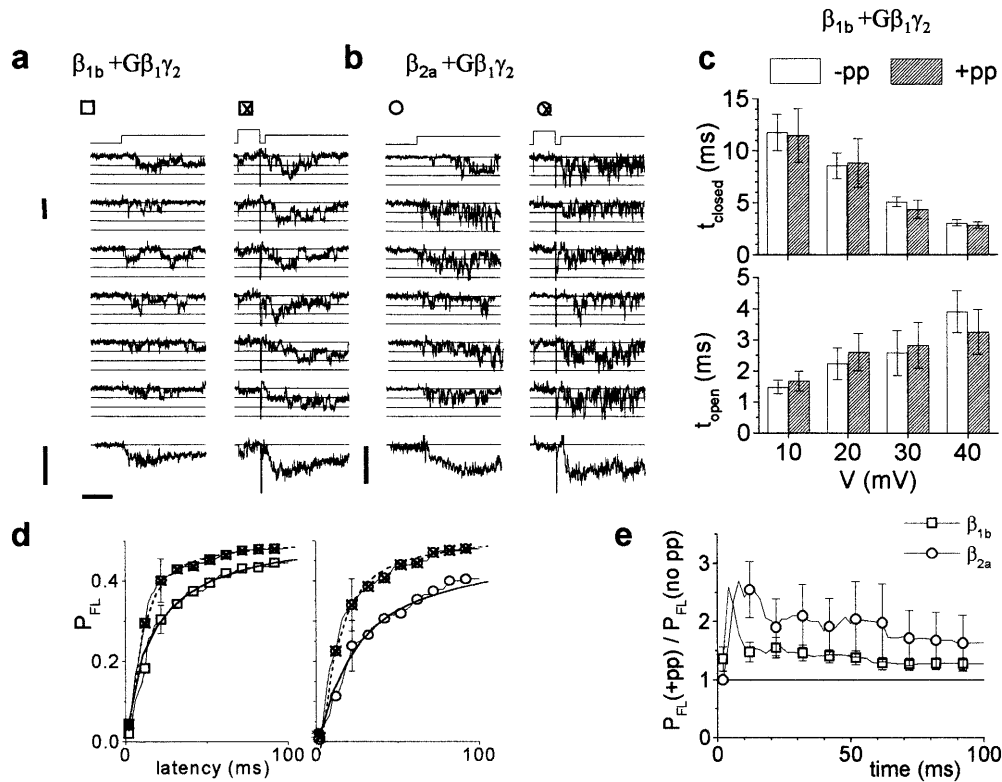
Fig. 7a–e Large brief prepulse facilitates $G\beta_1\gamma_2$-modulated Ca_v channels. **a** An example of a patch co-expressing $Ca_v2.2/\beta_{1b}$ and $G\beta_1\gamma_2$. *Top*: the voltage protocol: holding potential –100 mV and a pulse to +30 mV (*left*, no prepulse), or with prepulse (*right*), where the +30-mV pulse is preceded by a 40.ms pulse to +120 mV. The subsequent six episodes also demonstrate double and triple overlapping openings. The *bar* represents 1 pA. *Bottom*: ensembles of 20 (*left*) and 20 (*right*) episodes, the *scale bars* represent 0.5 pA and 50 ms. **b** An example of a patch co-expressing $Ca_v2.2/\beta_{2a}$ and $G\beta_1\gamma_2$. Format as in **a**. *Bottom*: ensembles of 15 episodes (*left*) and 20 (*right*) episodes. **c** Lack of influence of a prepulse on the mean closed (t_{closed}, *top*) and open (t_{open}, *bottom*) times at different voltages ($n=14$ with no prepulse, $n=6$ with prepulse, format as in Fig. 2c). **d** P_{FL} functions of $Ca_v2.2/\beta_{1b}/G\beta_1\gamma_2$ (*left*) and $Ca_v2.2/\beta_{2a}/G\beta_1\gamma_2$ (*right*) without ($\square$ and $\bigcirc$ respectively) or with (*crossed square* and *crossed circle*, respectively) a prepulse. Means (shown every 10 ms for clarity) ±SEM (shown only for 20 ms) of paired data from ten (*left*) and five (*right*) experiments. The paired data were significantly different at 20 ms in both cases (paired Student's *t*-test, $P<0.05$). The P_{FL} plots were fitted with a double exponential function (see text for details). **e** The rate of facilitation as assessed by dividing the P_{FL} plots with a prepulse by the result from the same experiment without a prepulse, generated from the same sets of data as in **d**

fected COS-7 cells. We compared the behaviour of $Ca_v2.2$ channels assembled with different subunit compositions and in the absence or presence of $G\beta_1\gamma_2$. Previously, we have reported that the β-subunit is required for the exhibition of many features of $G\beta_1\gamma_2$ modulation [30]. Here we extended this study by comparing the kinetic parameters and features of G protein modulation enforced on a $Ca_v2.2$ channel by two different auxiliary β-subunits. Co-expression of a β-subunit influenced many of these parameters strongly (see below). However, a detailed comparison between particular β-subunit

isoforms indicated that both influence most of these parameters similarly. To our knowledge, this is the first such comparison at the single-channel level. In addition, we confirmed that the main difference after co-expression of β_{2a} or β_{1b} is in the inactivation behaviour of the channels.

These comparisons are valuable since N-type channels with both β-isoforms are believed to be involved in transmitter release and subjected to $G\beta\gamma$ modulation. $Ca_v2.2$ channels are involved in transmitter release in many regions of the nervous system and in secretory cells. In the brain, only a small proportion of endogenous $Ca_v2.2$ interacts with the β_{2a}-subunit [41]. However, for chromaffin cells it has been proposed that $Ca_v2.2/\beta_{2a}$ channels form the non-inactivating N-type current and may contribute to hormone release [8]. However, N-type contribution to secretion in these cells is relatively small [1]. Early in development, $Ca_v2.2$ mainly associates with β_{1b}, but a significant proportion of N-type channels in adult rat brain also contains β_{1b}-subunits [51]. The N-type single-channel kinetic parameters (t_{open} and t_{closed}) are comparable with those reported in other studies, both in expression systems [52], and in native cells [28]. The latter shows a very similar voltage dependence for these parameters to that estimated here. Our data demonstrate that kinetic behaviour and G protein modulation (with this specific $G\beta\gamma$ combination) of N-type channels are the same, regardless of the β-subunit that regulates the inactivation properties of the channels.

Effects of the auxiliary β-subunit and differences between β_{1b} and β_{2a}

Although RT-PCR has detected endogenous mRNA for certain β subunits in COS-7 cells, expression of the protein is very low or absent [30]. We therefore treated the channels recorded as homogenous populations according to the β-subunit that was included in the transfection cocktail. The expression of a β-subunit modifies several aspects of Ca_v channel behaviour. $Ca_v2.2$ channels expressed with either β_{1b}- [52] or β_{2a}- [30] subunits show an increase in the mean channel t_{open}, compared with channels lacking this auxiliary subunit. In addition, shorter latency and reduction in nulls [30] accounts for the major part of the negative voltage shift in activation caused by β-subunits [53]. β-Subunits also alter the magnitude and kinetics of inactivation. However, this effect is heavily dependent on the β-isoform. β_1-, β_3- and β_4-subunits increase the inactivation magnitude by shifting the steady-state inactivation relationship to more hyperpolarised potentials while the β_{2a}-isoform shifts the voltage dependence of inactivation to more depolarised potential [11].

In the present study we found no differences in single-channel amplitude or mean t_{open} or t_{closed} between β_{1b}- and β_{2a}-subunits (Table 1, Fig. 2c and e). The activation process of $Ca_v2.2$ channels with these two subunits is very similar (Table 1 and Fig. 3c and d), apart from an additional slow activation phase seen with the β_{2a}-subunit (Fig. 3e). The slow activation phase appears to replace the relatively large null fraction occurring with the β_{1b}-subunit. The main parameter that distinguishes the two subunits is their ability to induce inactivation (Figs. 4, 5 and 6).

The β-subunit isoform influences inactivation

The time course of the development of inactivation varies depending on the experimental conditions and the methods used to examine it. In general it consists of a fast process in the range 50–500 ms (for review see [47]) and a slow process that takes more than 1 s to develop. In addition, some reports have described a fraction of the inactivation that takes more than 30 s to develop [43].

In terms of methodology, most of the experiments and analyses designed to explore inactivation have used a prepulse to induce inactivation. In this case the duration of the prepulse has a great influence on the extent of the inactivation measured. Other examinations of the inactivation process in single L-type channel records have used the latency-to-first-opening, FL, during a test pulse as a measure of prepulse-induced inactivation [26]. In T-type channels, ensemble current reconstruction is possible using FL and the burst duration [15], with termination of the burst describing the inactivation process. We investigated inactivation both by examining the effect of a prepulse and using the P_{LC} function instead of the burst duration.

β_{1b} or β_{2a} auxiliary subunits confer different inactivation properties on $Ca_v2.2$ channels. With the β_{1b}-subunit, steady-state inactivation is detected at depolarised potentials (Figs. 4 and 5) and inactivation during the test pulse exhibited a fast component ($\tau_{inact-fast}$ ~100–200 ms) and a slow component ($\tau_{inact-slow}$ ~1 s) (Fig. 6). With the β_{2a}-subunit, there was no significant steady-state inactivation (Figs. 4 and 5) and inactivation during the test pulse had no fast component but only a very slow component ($\tau_{inact-slow}$ ~5 s). These differences in inactivation properties conferred by the two β-subunits are similar to those published previously [11, 45]. With both β-subunits the inactivation profiles were similar with βARK_1 or $G\beta_1\gamma_2$ (Figs. 4d and 5a and b). Our results are in agreement with measurements of steady-state inactivation for control and transmitter-inhibited N-type currents demonstrating very little influence of G protein-mediated inhibition on the inactivation process (with the voltage dependence shifting in opposite directions in the different studies) [3, 22, 49]. It is notable, however, that the steady-state inactivation is directly related to loss of opening capability and is probably directly related to inactivation during the prepulse (Fig. 4a, right, episode 2 and Fig. 4b, right, episodes 1–4). This point is demonstrated further by the possibility of documenting steady-state inactivation from P_{FL} plots during the test pulse (Fig. 5).

Effects of co-expression of Gβγ

COS-7 cells have endogenous G protein components such as $G\alpha_z$ and $G\alpha_{12}$ [4], as well as $G\alpha_s$ [38], $G\alpha_q$ [55] and pertussis toxin-sensitive $G\alpha_{o/i}$ [54]. All the functional literature points to the fact that these G proteins exist as heterotrimers with Gβγ subunits and require receptor activation. Inclusion of the βARK1 Gβγ-binding domain is believed to remove any endogenous free Gβγ and, therefore, any G protein-related modulation. In contrast, inclusion of Gβγ induces permanently modulated Ca_v populations. The main inhibitory effect of $G\beta_1\gamma_2$ on $Ca_v2.2$ channels containing either β_{1b}- or β_{2a}-subunits was on the activation process (Table 1 and Fig. 3). P_{FL} values decrease both because of kinetic slowing and as a result of the large increase in the null fraction. At +40 mV the null fraction increased by ~20%, at the expense of the fast component of activation, with both β-isoforms. In both cases the fast time constant for activation was slowed from ~10 to ~20 ms. The increase in the null fraction did not recover (Fig. 3e) with a 2-s pulse that would have uncovered late openings. These results are in complete agreement with a study on native N-type channels [13], although another study has reported recovery within 400 ms [35]. G protein modulation of $Ca_v2.2$ channels depended very little on the β-subunit species, although minor differences in the activation slowing and in facilitation were detected.

At +40 mV, $G\beta_1\gamma_2$ also caused an increase in the mean t_{closed}. The differences in t_{closed} between βARK_1-

and $G\beta_1\gamma_2$-co-transfected cells were restricted to this voltage (Fig. 2c and e). The increase in t_{closed} suggests a mechanism by which, in addition to the kinetic slowing of activation, $G\beta\gamma$ also has an influence on the channel properties after the channel has activated (first opening after latency). These results are in agreement with the suggestion that "reluctant", or $G\beta\gamma$-bound, channels open only at large depolarisations and result in a low-P_{open} behaviour including an additional long closed state [28].

Relief of $G\beta\gamma$ modulation in $G\beta_1\gamma_2$-modulated channels was examined by assessing the facilitation by a short, strong prepulse. This process was similar with both β-subunits. Facilitation consisted mainly of enhancement of $\tau_{act\text{-}fast}$, usually leading to a decrease of the null fraction but not of t_{closed} (Fig. 7, see also [13]). This suggests that during the prepulse, a degree of reluctant gating is initiated, and it implies further that such a prepulse does not remove all the bound $G\beta\gamma$.

N-type channels constructed with one of two different β-subunit isoforms differed in their inactivation behaviour. This is probably due to an N-terminal palmitoylation of the β_{2a}-isoform, which contributes to the low ability of this subunit to induce inactivation of these channels [11]. However, this structural difference does not influence the ability of an auxiliary β-subunit to enhance other kinetic parameters and allow voltage-dependent modulation of the channel by G proteins. These parameters were similar with both types of β-subunit isoform. These results further point to the delicate regulation of calcium signals by means of local expression and assembly of the Ca_v channel proteins and their interactions with other proteins.

References

1. Artalejo CR, Mogul DJ, Perlman RL, Fox AP (1991) Three types of bovine chromaffin cell Ca^{2+} channels: facilitation increases the opening probability of a 27 pS channel. J Physiol (Lond) 444:213–240
2. Atlas D (2001) Functional and physical coupling of voltage-sensitive calcium channels with exocytotic proteins: ramifications for the secretion mechanism. J Neurochem 77:972–985
3. Bean BP (1989) Neurotransmitter inhibition of neuronal calcium currents by changes in channel voltage-dependence. Nature 340:153–155
4. Belcheva MM, Wong YH, Coscia CJ (2000) Evidence for transduction of mu but not kappa opioid modulation of extracellular signal-regulated kinase activity by G(z) and G(12) proteins. Cell Signal 12:481–489
5. Bichet D, Cornet V, Geib S, Carlier E, Volsen S, Hoshi T, Mori Y, De Waard M (1999) The I-II loop of the Ca^{2+} channel alpha(1) subunit contains an endoplasmic reticulum retention signal antagonized by the beta subunit. Neuron 25:177–190
6. Brice NL, Berrow NS, Campbell V, Page KM, Brickley K, Tedder I, Dolphin AC (1997) Importance of the different β subunits in the membrane expression of the $\alpha 1A$ and $\alpha 2$ calcium channel subunits: studies using a depolarisation-sensitive $\alpha 1A$ antibody. Eur J Neurosci 9:749–759
7. Burgess DL, Davis CF, Gefrides LA, Noebels JL (1999) Identification of three novel Ca^{2+} channel gamma subunit genes reveals molecular diversification by tandem and chromosome duplication. Genome Res 9:1204–1213
8. Cahill, AL, Hurley JH, Fox AP (2000) Coexpression of cloned alpha(1B), beta(2a), and alpha(2)/delta subunits produces non-inactivating calcium currents similar to those found in bovine chromaffin cells. J Neurosci 20:1685–1693
9. Campbell V, Berrow N, Brickley K, Page K, Wade R, Dolphin AC (1995) Voltage-dependent calcium channel β-subunits in combination with alpha1 subunits have a GTPase activating effect to promote hydrolysis of GTP by G alpha$_o$ in rat frontal cortex. FEBS Lett 370:135–140
10. Canti C, Davies A, Berrow NS, Butcher AJ, Page KM, Dolphin AC (2001) Evidence for two concentration-dependent processes for β subunit effects on $\alpha 1B$ calcium channels. BiophysJ 81:1439–1451
11. Canti C, Bogdanov Y, Dolphin AC (2000) Interaction between G proteins and accessory beta subunits in the regulation of alpha1B calcium channels in *Xenopus* oocytes. J Physiol (Lond) 527:419–432
12. Canti C, Page KM, Stephens GJ, Dolphin AC (1999) Identification of residues in the N-terminus of $\alpha 1B$ critical for inhibition of the voltage-dependent calcium channel by $G\beta\gamma$. J Neurosci 19:6855–6864
13. Carabelli V, Lovallo M, Magnelli V, Zucker H, Carbone E (1996) Voltage-dependent modulation of single N-type Ca^{2+} channel kinetics by receptor agonists in IMR32 cells. BiophysJ 70:2144–2154
14. Cens T, Restituito S, Galas S, Charnet P (1999) Voltage and calcium use the same molecular determinants to inactivate calcium channels. J Biol Chem 274:5483–5490
15. Chen C, Hess P (1990) Mechanism of gating of T-type calcium channels. J Gen Physiol 96:603–630
16. Chien AJ, Zhao XL, Shirokov RE, Puri TS, Chang CF, Sun D, Rios E, Hosey MM (1995) Roles of a membrane-localized β subunit in the formation and targeting of functional L-type Ca^{2+} channels. J Biol Chem 270:30036–30044
17. Colquhoun D, Hawkes AG (1990) Stochastic properties of ion channel openings and bursts in a membrane patch that contains two channels: evidence concerning the number of channels present when a record containing only single openings is observed. Proc R Soc Lond [Biol] 240:453–477
18. Cormack BP, Valdivia RH, Falkow S (1996) FACS-optimized mutants of the green fluorescent protein (GFP). Gene 173:33–38
19. Costantin J, Noceti F, Qin N, Wei XY, Birnbaumer L, Stefani E (1998) Facilitation by the β_{2a} subunit of pore openings in cardiac Ca^{2+} channels. J Physiol (Lond) 507:93–103
20. Dolphin AC (1998) Mechanisms of modulation of voltage-dependent calcium channels by G proteins. J Physiol (Lond) 506:3–11
21. Dunlap K, Luebke JI, Turner TJ (1995) Exocytotic Ca^{2+} channels in mammalian central neurons. Trends Neurosci 18:89–98
22. Elmslie KS, Jones SW (1994) Concentration dependence of neurotransmitter effects on calcium current kinetics in frog sympathetic neurones. J Physiol (Lond) 481:35–46
23. Herlitze S, Garcia DE, Mackie K, Hille B, Scheuer T, Catterall WA (1996) Modulation of Ca^{2+} channels by G-protein βgamma subunits. Nature 380:258–262
24. Herlitze S, Hockerman GH, Scheuer T, Catterall WA (1997) Molecular determinants of inactivation and G protein modulation in the intracellular loop connecting domains I and II of the calcium channel α_{1A} subunit. Proc Natl Acad Sci USA 94:1512–1516
25. Ikeda SR (1996) Voltage-dependent modulation of N-type calcium channels by G protein βgamma subunits. Nature 380:255–258

26. Imredy JP, Yue DT (1994) Mechanism of Ca^{2+}-sensitive inactivation of L-type Ca^{2+} channels. Neuron 12:1301–1318
27. Jones SW (1998) Overview of voltage-dependent calcium channels. J Bioenerg Biomembr 30:299–312
28. Lee HK, Elmslie KS (1999) Gating of single N-type calcium channels recorded from bullfrog sympathetic neurons. J Gen Physiol 113:111–124
29. Letts VA, Felix R, Biddlecome GH, Arikkath J, Mahaffey CL, Valenzuela A, Bartlett FS, Mori Y, Campbell KP, Frankel WN (1998) The mouse stargazer gene encodes a neuronal Ca^{2+} channel gamma subunit. Nat Genet 19:340–347
30. Meir A, Bell DC, Stephens GJ, Page KM, Dolphin AC (2000) Calcium channel β subunit promotes voltage-dependent modulation of α1B by Gβγ. Biophys J 79:731–746
31. Meir A, Dolphin AC (1998) Known calcium channel α1 subunits can form low threshold, small conductance channels, with similarities to native T type channels. Neuron 20:341–351
32. Meir A, Ginsburg S, Butkevich A, Kachalsky SG, Kaiserman I, Ahdut R, Demirgoren S, Rahamimoff R (1999) Ion channels in presynaptic nerve terminals and control of transmitter release. Physiol Rev 79:1019–1088
33. Neher E (1995) Voltage offsets in patch-clamp experiments. In: Sakmann B, Neher E (eds) Single-channel recording. Plenum Press, New York, p 147
34. Page KM, Canti C, Stephens GJ, Berrow NS, Dolphin AC (1998) Identification of the amino terminus of neuronal Ca^{2+} channel α1 subunits α1B and α1E as an essential determinant of G protein modulation. J Neurosci 18:4815–4824
35. Patil PG, De Leon M, Reed RR, Dubel S, Snutch TP, Yue DT (1996) Elementary events underlying voltage-dependent G-protein inhibition of N-type calcium channels. Biophys J 71:2509–2521
36. Patlak J, Horn R (1982) Effects of *N*-bromoacetamide on single sodium channel currents in excised membrane patches. J Gen Physiol 79:333–351
37. Peterson BZ, DeMaria CD, Yue DT (1999) Calmodulin is the Ca^{2+} sensor for Ca^{2+}-dependent inactivation of 1-type calcium channels. Neuron 22:549–558
38. Rauly I, Alihaud M, Wurch T, Pauwels PJ (2000) α(2A)-adrenoceptor: G(αi1) protein-mediated pertussis toxin-resistant attenuation of G(s) coupling to the cyclic AMP pathway. Biochem Pharmacol 59:1531–1538
39. Roche JP, Treistman SN (1998) The calcium channel β3 subunit enhances voltage-dependent relief of G protein inhibition induced by muscarinic receptor activation and Gβ gamma. J Neurosci 18:4883–4890
40. Scott RH, Dolphin AC (1986) Regulation of calcium currents by a GTP analogue: potentiation of (–)-baclofen-mediated inhibition. Neurosci Lett 69:59–64
41. Scott VES, De Waard M, Liu HY, Gurnett CA, Venzke DP, Lennon VA, Campbell KP (1996) β Subunit heterogeneity in N-type Ca^{2+} channels. J Biol Chem 271:3207–3212
42. Shirokov R, Ferreira G, Yi JX, Ríos E (1998) Inactivation of gating currents of L-type calcium channels – specific role of the $α_2δ$ subunit. J Gen Physiol 111:807–823
43. Sokolov S, Weiß RG, Timin EN, Hering S (2000) Modulation of slow inactivation in class A Ca^{2+} channels by β-subunit. J Physiol (Lond) 527:445–454
44. Stephens GJ, Berrow NS, Page KM, Dolphin AC (1997) Gβgamma subunits mediate aspects of G protein sensitivity of Ca^{2+} sensitivity of calcium channel α1 subunits by an action on the I-II loop (abstract). J Physiol (Lond) 504:157P
45. Stephens GJ, Page KM, Bogdanov Y, Dolphin AC (2000) The α1B calcium channel amino terminus contributes determinants for β subunit mediated voltage-dependent inactivation properties. J Physiol (Lond) 525:377–390
46. Stephens GJ, Page KM, Burley JR, Berrow NS, Dolphin AC (1997) Functional expression of rat brain cloned α1E calcium channels in COS-7 cells. Pflugers Arch 433:523–532
47. Stotz SC, Zamponi GW (2001) Structural determinants of fast inactivation of high voltage-activated Ca^{2+} channels. Trends Neurosci 24:176–182
48. Swick AG, Janicot M, Cheneval-Kastelic T, McLenithan JC, Lane DM (1992) Promoter-cDNA-directed heterologous protein expression in *Xenopus laevis* oocytes. Proc Natl Acad Sci USA 89:1812–1816
49. Toselli M, Tosetti P, Taglietti V (1999) Kinetic study of N-type calcium current modulation by δ-opioid receptor activation in the mammalian cell line NG108-15. Biophys J 76:2560–2574
50. Tsien RW, Ellinor PT, Horne WA (1991) Molecular diversity of voltage-dependent Ca^{2+} channels. Trends Pharmacol Sci 12:349–354
51. Vance CL, Begg CM, Lee WL, Haase H, Copeland TD, McEnery MW (1998) Differential expression and association of calcium channel $α_{1B}$ and β subunits during rat brain ontogeny. J Biol Chem 273:14495–14502
52. Wakamori M, Mikala G, Mori Y (1999) Auxiliary subunits operate as a molecular switch in determining gating behaviour of the unitary N-type Ca^{2+} channel current in *Xenopus* oocytes. J Physiol (Lond) 517:659–672
53. Walker D, De Waard M (1998) Subunit interaction sites in voltage-dependent Ca^{2+} channels. Trends Neurosci 21:148–154
54. Wurch T, Pauwels PJ (2001) Coupling of canine serotonin 5-HT(1B) and 5-HT(1D) receptor subtypes to the formation of inositol phosphates by dual interactions with endogenous G(i/o) and recombinant G(α15) proteins. J Neurochem 75:1180–1189
55. Yuan J, Slice L, Walsh JH, Rosengurt E (2001) Activation of protein kinase D by signaling through the alpha subunit of the heterotrimeric G protein G(q). J Biol Chem 275:2157–2164
56. Zhang J-F, Ellinor PT, Aldrich RW, Tsien RW (1994) Molecular determinants of voltage-dependent inactivation in calcium channels. Nature 372:97–100